

A SUPERCONDUCTING MAGNETIC SHIELD FOR THE PHOTOELECTRON INJECTOR OF bERLinPro

J. Völker *, A. Frahm, A. Jankowiak, S. Keckert, J. Knobloch,
G. Kourkafas, O. Kugeler, A. Neumann, H. Plötz
Helmholtz Zentrum Berlin, Berlin, Germany

Abstract

Magnetic fields are a big issue for SRF cavities, especially in areas with strong electromagnets or ferromagnetic materials. Magnetic shieldings consisting of metal alloys with high magnetic permeability are often used to reroute the external magnetic flux from the cavity region. Those Mu metal shields are typically designed for weak magnetic fields like Earth's magnetic field. Next to strong magnetic field sources like superconducting (SC) solenoids, those shields can be easily saturated, resulting in a degradation of the shielding efficiency and a permanent magnetization. For the photoinjector of bERLinPro a new SC solenoid will be installed inside the cryomodule next to the SRF gun cavity. Calculations show that the fringe fields of the solenoid during operation can saturate the cavity Mu-metal shields. Therefore we designed an SC magnetic shield placed between the solenoid and the cavity shield to protect the latter during magnet operation. In this paper we will present the design and first testings of this SC magnetic shield.

INTRODUCTION

bERLinPro [1] is the Energy recovery linac (ERL) project under construction at HZB. For this accelerator electron bunches are extracted inside the injector module from a semiconductor photocathode by a pulsed drive laser. The removable photocathode is placed next to the backwall of the 1.4-cell SRF gun cavity. After extraction from the cathode the electrons bunches are accelerated in the 1.3 GHz field of the gun cavity. Further components in the injector module are the cathode transfer system, a superconducting solenoid, a HOM absorber and some orbit corrector magnets for beam adjustment. The solenoid magnet is the first focussing magnet downstream the gun cavity and it is essential for the beam performance of the whole ERL due to the emittance compensation and the symmetrical beam focussing. The magnetic field of the solenoid produces a rotation and an overall focussing of the beam as a function of the integrated field strength depending on the electric current in the coil. The shape of the longitudinal field profile defines also the nonlinear focussing and rotation effects in the beam (aberration effects). To minimize these effects, the field profile has to be as long and smooth as possible. For the new solenoid magnet for bERLinPro (see Fig. 1), the magnet geometry was optimized to combine a minimal aberration field profile with improved electrical and cooling parameters for a more stable operation. Additionally to an optimal field profile of

the magnet, the longitudinal position is relevant. For minimum transverse emittance values the solenoid has to be placed as close as possible to the exit of the gun cavity. The combination of a long field profile and a short distance to the gun cavity produces a huge amount of fringe fields in the area of the SRF gun.

The SRF gun for bERLinPro has two magnetic shieldings consisting of metal alloys with high magnetic permeability to guide external magnetic fields around the sensitive area of the cavity. They are designed for low field strength in the range of the Earth magnetic field. The relative magnetic permeability (μ_r) of those shields can have values up to 300 000 but only for a small magnetic field strength [2]. In case of high field strength they can be easily saturated, resulting in flux densities of ≈ 0.85 T inside the material. To protect those shields for a magnetization and a degradation of the shielding efficiency, the inner flux density in the metal alloy should be as small as possible. Such a protection can be a diamagnetic plate between the magnetic source and the Mu shield, e.g. a superconducting plate. The necessary calculations were done together with the optimisaton of the new solenoid magnet.

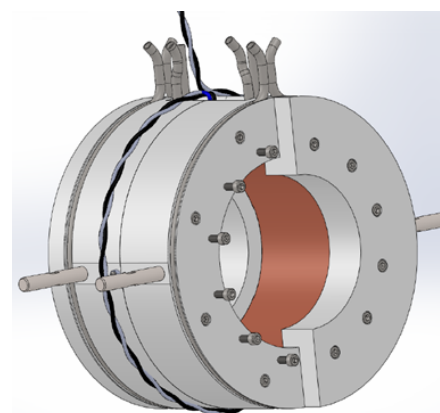


Figure 1: Sketch of the new solenoid for the bERLinPro photoinjector.

SOLENOID

Due to an apparent short-circuit in the initial solenoid [3] a new magnet should be designed and bought. Based on the existing magnet design, some modification should be done to minimize the risk of another magnet damage (for important parameters of the old and the new version of the solenoid see Table 1).

Those are:

- reduction of the magnet inductivity

* jens.voelker@helmholtz-berlin.de

- use of more robust wires with an increased ratio of Cu to NbTi (less ohmic losses in case of a quench)
- an additional electric insulation layer between coil and the Cu winding bobbin
- a direct cooling of the Cu bobbin for a redundant cooling of the superconducting coil in any case
- displacement of the cooling lines in the yoke from a region with a high magnetic flux density to achieve a smoother magnetic flux gradient inside the yoke material
- a more flexible yoke design to change the magnetic field profile and the effective length (removable pole shoes)

The magnet design was worked out in collaboration with the company Niowave [4] which also constructed it. The final magnet was tested afterward at HZB. Especially the effects of the geometry changes on the magnetic profile were studied as well as the magnetic interaction with adjacent regions for all steps of the design process. Most of these field calculations were done with the field solver SuperFish [5]. However for non-rotationally symmetrical problems also CST was used. Thereby it was observed that one of the important interactions is between the solenoid and the several Mu shield next to it.

Table 1: Important parameters of the old and the new version of the solenoid. The solenoid values without pole shoes are shown in parenthesis.

parameter	Solenoid1.0	Solenoid2.0
yoke size (mm)	136.5 x 258.2	174 x 261.2 (136.1 x 261.2)
coil size (mm)	70 x 17.23	70 x 19.67
windings	8368	3030
inductivity (H)	27	2.8 (2.6)
cooling	only pole shoes / yoke edges	coil and return yoke
effective mag. length (mm)	83.33	92.49 (99.47)
Mu shield	yes	no

CALCULATION OF THE MAGNETIC FIELD DISTRIBUTION NEXT TO THE SOLENOID

For the calculation of the magnetic field distribution next to the solenoid, the geometry of the magnet and other magnetically sensitive components, like the Mu shields, were implemented in the field solver. For different coil current settings of the solenoid, the magnetic flux density in the magnet and those components were calculated. All materials were defined with variable magnetic permeability curves. Especially for the Mu shields a data set of measured high permeability metal alloys at cryogenic temperatures were used. Figure 2 shows three measured hysteresis curves of those materials (Cryoperm and MuMetal).

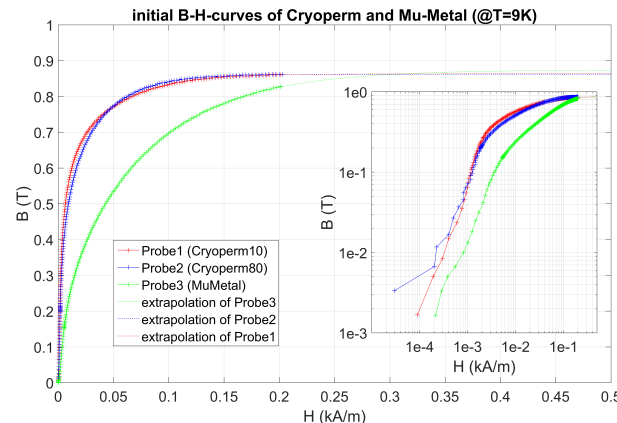


Figure 2: Initial hysteresis curves of three high permeability metal alloys at 9K temperature (measured data by O. Kugeler, HZB).

During the design process for the new solenoid the detailed calculations with these real hysteresis curves revealed a feature in the existing solenoids for bERLinPro photoinjector guns (for gun0 and the solenoid 1.0). Both magnets were designed with an external Mu-shield around the yoke, which should suppress the magnetic field outside the solenoid resulting by the residual fields of the magnet yoke. However, they are mainly used as another thin yoke once the coil is powered up. This produces high magnetic flux density values inside the Mu metal alloy up to the saturation limit. On the other hand, such a Mu shield around the solenoid has in best case only a small shielding efficiency in the adjacent magnetic sensitive areas, like the gun cavity, in the range of 30 %. As an example, each Mu shield of the gun cavity suppress the residual magnetic field of the yoke by a factor of 99 %. Therefore an additional Mu shield for the solenoid magnet is not useful.

Furthermore these calculations can be used to observe the load of the cavity Mu shields (Cryoperm) during solenoid operation. A simplified model of the inner and outer cavity shieldings are implemented in Superfish next to the new solenoid geometry. Figure 3 and Fig. 4 show a radial cut of this setup with coil, Cu winding bobbin, the main return yoke and the Mu metal shields of the gun cavity together with the calculated flux density values as color code. In this example, the areas with the highest magnetic flux density are the yoke of the solenoid and the front of the outer cavity Mu shield. For an analysis of the flux densities inside the shield material in more detail, these values were sampled along the path s (see Fig. 4) for different solenoid current values I_{sol} in 5 Amp steps up to 30 Amp (Fig. 5). The maximum operation current of the solenoid is 20 Amp. Especially in the front plate of the outer Mu shield high magnetic flux density values were achieved up to the saturation limit of the material (red zone). The yellow zone in Fig. 5 marks the region with the non-linearity in the hysteresis curve and with starting magnetization processes of such a high permeability material. Even for standard operation currents of the

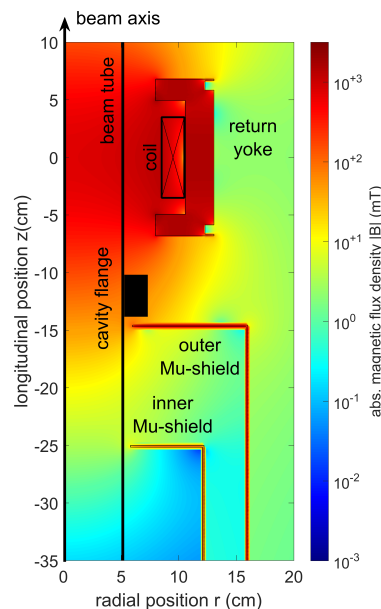


Figure 3: Radial cut of the geometry next to the solenoid. Here, the electron beam propagates from bottom to top at $r=0$, the beam axis.

solenoid between 5 Amp and 15 Amp the load of the Mu shield is in this non linear range.

To reduce these high values inside the material, the cavity shielding has to be at least 3 time thicker as the existing metal alloy, which is quite expensive and quite complicated for the existing shield geometry. One way to protect the outer Mu shield of the gun is a deflecting shield between the solenoid and the Mu material consisting of a superconducting plate. This works as a perfect diamagnet during the solenoid operation and blocks the extreme magnetic field values of the magnet (Meissner effect). Therefore a thin superconducting metal alloy like niobium will be placed next to the outer shield with similar dimension as its front plate. Most of the magnetic field will flow in front of the superconductor and only a small fraction will go through the beam pipe opening and enter the Mu shield. This can be seen in Fig. 6, which shows the calculation results for this setup. Here, a quasi-perfect diamagnetic material ($\mu_r = 10^{-10}$) with a thickness of 1.5 mm and an outer diameter of 300 mm is implemented in the given geometry shown in Fig. 3 with a distance of 8 mm in front of the outer Mu shield. As long as the magnetic flux density next to the superconductor keeps below a critical values the plate deflects the magnetic field and only a small fraction enters the mu metal.

The calculations of different geometry setups show that the SC shield needs to have nearly the same diameter and has to be placed as near as possible to the outer Mu shield. In this case (Fig. 6) the maximum flux density value stays below the critical saturation limit of the Cryoperm material for all coil currents. A critical point of this SC shield is the flux density next to the superconductor itself. To avoid a quench of the niobium plate during operation, the field

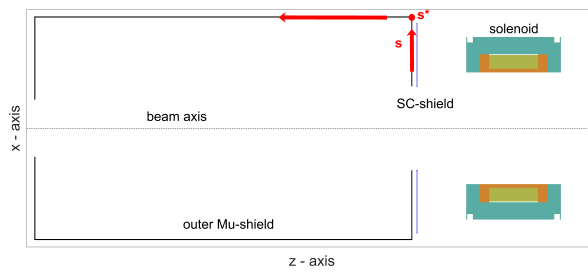


Figure 4: Cut through the calculated geometry and definition of the path line s for the magnetic flux density analysis.

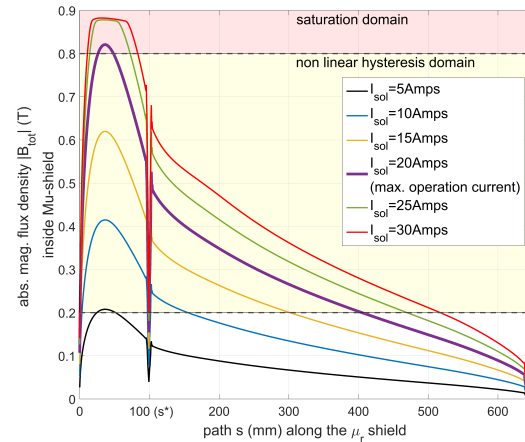


Figure 5: Magnetic flux density inside the cavit's outer Mu metal alloy along the path s for different coil current values.

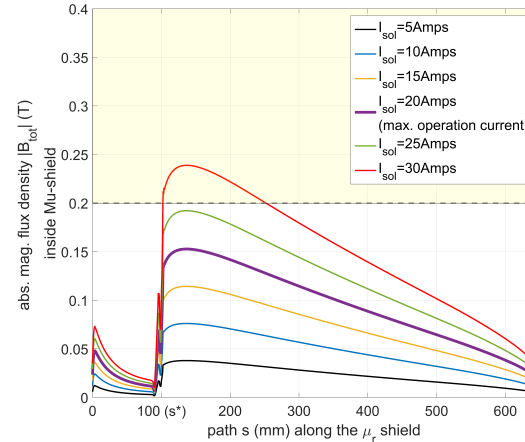


Figure 6: Magnetic flux density inside the cavity's outer Mu metal alloy along the path s for different coil current values. Here, the Cryoperm material was shielded by an SC shield. The yellow region marks the same non linear hysteresis domain as shown in Fig. 5.

has to be less than ≈ 198 mT (at absolute zero) [6]. According to the Superfish simulations the maximum field value next to the superconductor was determined to ≈ 80 mT for $I_{sol} = 30$ Amp, which should be not a problem.

Further detailed calculations based on CST are in progress. Therefore the final setup and the original geometries were implemented (Fig. 7), but result in a huge discrepancy of

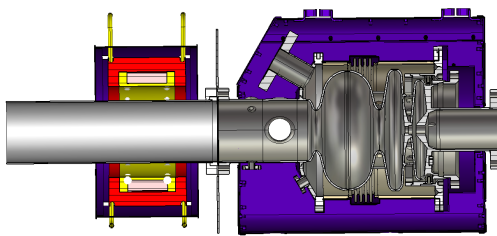


Figure 7: Sketch of the complete module setup for first calculations with CST. From right to left: Gun Cavity with Cathode insertion, inner and outer (blue) magnetic shield. SC shield directly on the flange → for the current design, the niobium plate is right of the flange. Solenoid with its red marked yoke.

the necessary mesh setup between the big setup in total and the thin structures of the curved shielding alloys. Up to now it was not possible to find a computable mesh setting which results in physically correct field distributions.

DESIGN OF THE SC SHIELD

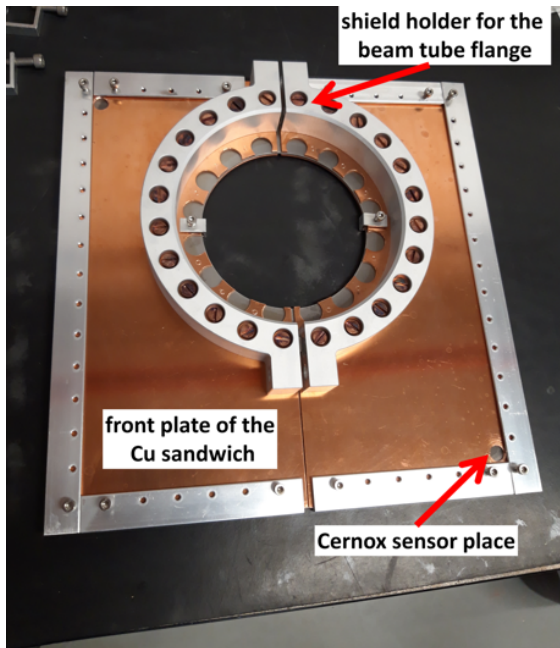


Figure 8: first SC shield construction for the test in the bERLinPro gun module

The superfish calculation showed that the superconducting shield needs to have a diameter of nearly the same size as the Cavity shield to protect also the edges. Therefore a 300 mm × 300 mm × 1.5 mm niobium plate is used which can be installed between the Gun shield and the solenoid. The plate is fixed between two Cu-plates with the same size, which provide a uniform cooling of the superconductor. These three layers were pressed together with clamps all around. The final shield consists of two symmetric pieces to mount it on the beam tube between the solenoid and the cavity. A half ring was welded on each of the plates as clamp connector for the beam line flange which has nearly the same

temperature as the gun cavity inside the liquid helium bath (2 K). Thus the clamp ring works also as cooler for the SC shield. Figure 8 shows this shield design as it was used for the first module test.

FIRST TEST OF THE SC SHIELD

To test this design the shield was installed together with the new solenoid and a dummy beam tube in the bERLin-Pro gun module (Fig. 9). Several hall sensors were placed around the SC shield and inside the solenoid to measure the field distribution which can be compared with the field calculations. Figure 10 shows a sketch of the module setup as a longitudinal cut. Six 1D-Hall sensors are placed on both sides from the SC shield and measure the radial field component (violet arrows).

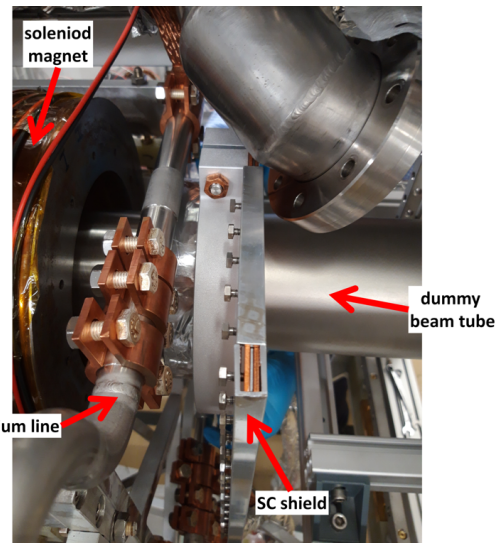


Figure 9: picture of the first test setup inside the gun cryostat.

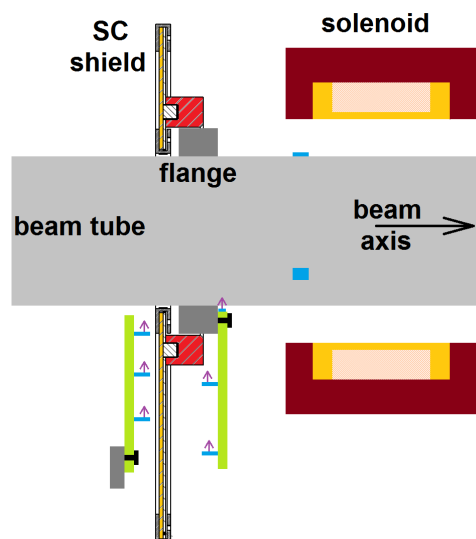


Figure 10: Scheme of the solenoid and SC shield setup for the module test.

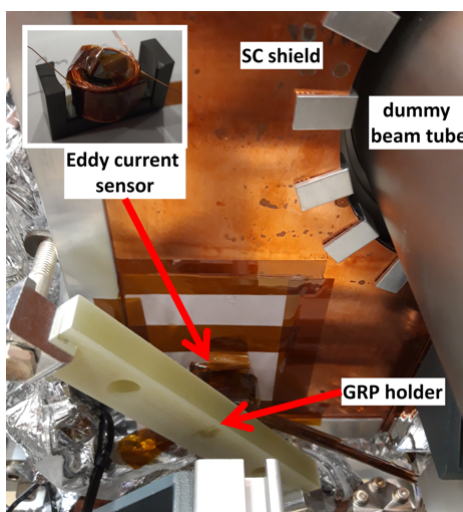


Figure 11: Picture of the installed Eddy-current sensor. The sensor is fixed on the shield by a dielectric holder consisting of glass-fibre reinforced plastic (GRP).

Another three sensors are placed on the beam tube and were used for further solenoid tests and calibrations. Additionally a low frequency Eddy current sensor was connected to the backside of the shield (Fig. 11) to determine the change of the ohmic resistance during cool down. The sensitivity of this sensor depends on the used frequency. For this test a frequency of 30 Hz was used to visualize small ohmic values and especially the superconducting transition of the shield.

In this test setup the dummy beam tube cannot be cooled by the helium bath of the gun cavity. To compensate this, the dummy tube and the shield were connected to 4 K He lines and the two-phase vessel by several copper strands. Unfortunately the combination of the cooling mechanism and a leakage in the Helium system could not provide a cooling of the niobium plate below 15 K. The leakage of the 4 K helium system into the insulation vacuum during a helium pressure of 1 bar was big enough to interfere the turbo pump of the cryo module. However it was tolerable in case of the 1.8 K temperature mode with a helium pressure of only 16 mbar in the system. The temperature of the helium gas return pipe in this mode is not well defined and can achieve values of more than 10 K. It seems to be, that the temperature of the dummy beam tube was dominated by this quite high value of the helium gas return pipe, because of the reduced thermal conductivity of the Cu strands for lower temperatures as these connected to the 2 K He lines.

A second test of the SC shield is planned with a small cooling modification. The lateral clamps were extended to connect directly a He tube with a diameter of 8 mm on

the shield. This additional line can be connected in series with the superconducting solenoid, cooled down to 5 K by overcritical helium.

CONCLUSION

It is important to analyze the interaction of strong electromagnets with magnetic sensitive materials especially in compact cryo modules where a superconducting solenoid is used. In case of high magnetic permeability metal alloys used as magnetic shielding, the additional fringe fields of such a magnet can produce magnetic flux density values in the material up to the saturation. Calculation of the complete magnetically relevant setup are necessary to define positions and dimensions, but also to observe the effectiveness of such a shield. It could be shown for the injector module of bERLinPro, that a magnetic shield around the solenoid magnet is not efficient for the protection of an SRF gun cavity next to it, in relation to a magnetic shield around the cavity. However, even those shield materials can be affected by the magnet fringe fields. One option which was shown in this paper is the use of a superconducting shield next to high magnetic permeability alloy metals. It deflects most of the magnetic flux and protects the cavity shields during solenoid operation. The principle and the design of such a superconducting shield were presented. Unfortunately, it was not possible during the first test to achieve the superconducting state of the niobium shield. Another test with improved shield cooling is planned.

REFERENCES

- [1] A. Jankowiak, M. Abo-Bakr, W. Anders, A.B. Büchel, K.B. Bürkmann-Gehrlein, P. Echevarria, *et al.*, "Status of the Berlin Energy Recovery Linac Project BERLinPro", presented at ERL'17, Geneva, Switzerland, Jun 2017, paper WEIACC002, unpublished.
- [2] M. Masuzawa, A. Terashima, K. Tsuchiya, A. Dael, O. Napol, and J. Plouin, "Magnetic Shielding: Our Experience with Various Shielding Materials", in *Proc. SRF'13*, Paris, France, Sep. 2013, paper WEIOD02, pp. 808–811.
- [3] A. Neumann *et al.*, "The bERLinPro SRF Photoinjector System - From First RF Commissioning to First Beam", in *Proc. IPAC'18*, Vancouver, Canada, Apr.-May 2018, pp. 1660–1663.
doi:10.18429/JACoW-IPAC2018-TUPML053
- [4] Niowave Inc., <https://www.niowaveinc.com/>
- [5] Poisson Superfish, https://laacg.lanl.gov/laacg/services/download_sf.phtml
- [6] C. Kittel, "Introduction to Solid State Physics", 7th Ed., Wiley, 1996.